Available online at www.sciencedirect.com
ScienceDirect
Journal of the European Ceramic Society 31 (2011) 2407–2414
www.elsevier.com/locate/jeurceramsoc

On the crystallite size refinement of ZrB_2 by high-energy ball-milling in the presence of SiC

V. Zamora [a], A.L. Ortiz [a,*], F. Guiberteau [a], M. Nygren [b], L.L. Shaw [c]

[a] *Departamento de Ingeniería Mecánica, Energética y de los Materiales, Universidad de Extremadura, 06006 Badajoz, Spain*
[b] *Department of Materials and Environmental Chemistry, University of Stockholm, 10691 Stockholm, Sweden*
[c] *Department of Chemical, Materials and Biomolecular Engineering, University of Connecticut, Storrs, CT 06269, USA*

Received 9 March 2011; received in revised form 14 May 2011; accepted 25 May 2011
Available online 25 June 2011

Abstract

The effect of SiC addition (5, 17.5, and 30 vol.%) on the high-energy ball-milling (HEBM) behaviour of ZrB_2 is investigated. It was found that the presence of SiC during HEBM did not alter ZrB_2 refinement mechanism of repeated brittle fracture followed by cold-welding, thereby leading to the formation of agglomerates consisting of primary nano-particles. SiC did, however, slow down the kinetics of crystallite size refinement and promoted the formation of finer agglomerates. Both of these phenomena became more pronounced with increasing SiC content in the ZrB_2 + SiC powder mixtures, and they were attributed to the energy dissipation effect of the nanocrystalline SiC particles during HEBM of the ZrB_2 + SiC powder mixture. This study offers the first evidence that the addition of harder materials to softer materials can slow down the refinement of crystallite sizes, and thus provides a new mechanism to control crystallite sizes during HEBM. The simultaneous attainment of nano-particles of ZrB_2 and SiC, reduced agglomerate sizes, and homogeneous SiC dispersion at the nanometre scale may have important implications for the ultra-high-temperature ceramic community, as it simplifies the processing route and is likely to facilitate the sintering of ZrB_2–SiC composites.

Keywords: ZrB_2; Ultra-high-temperature ceramics; High-energy ball-milling; Comminution

1. Introduction

The ultra-high-temperature ceramic (UHTC) ZrB_2 is currently being actively investigated as an aerospace material for extreme environments such as those encountered in hypersonic flights, atmospheric re-entry, and rocket propulsion. However, ZrB_2 is not only hard to sinter,[1,2] but also by itself does not meet all the exigent requirements of oxidation resistance and mechanical properties demanded by extreme-environment aerospace engineering.[1,2] For these reasons, ZrB_2 is typically combined with other refractory ceramics. One of the most widely used is SiC at relative concentrations between 5 and 30 vol.%.[1,2] The benefit of adding SiC to ZrB_2 is threefold. Firstly, SiC acts as a sintering aid, facilitating densification at lower temperatures. This is attributed to the fact that the surface of the SiC particles is covered by a thin film of SiO_2 that promotes liquid-phase sintering.[3] Secondly, SiC provides ZrB_2 with greater oxidation and ablation resistance because the borosilicate scales resulting from the simultaneous oxidations of ZrB_2 and SiC are much more protective than the boria scales resulting from the oxidation of ZrB_2 alone.[1,2] Thirdly, SiC improves the (thermo-)mechanical properties relevant for the aerospace applications proposed for ZrB_2.[1,2] For example, the hardness increases because SiC is harder than ZrB_2, the toughness improves because of the crack defection and crack-wake bridging in the weak ZrB_2–SiC interfaces, the strength increases because SiC inhibits grain growth thus reducing the dominant initial flaw size, and finally, the thermal shock resistance also improves since SiC increases the strength and thermal conductivity, and lowers the elastic modulus of the composite. It is not surprising therefore that more research effort is being devoted to the development of ZrB_2 + SiC UHTCs than of ZrB_2 UHTCs.

Current practice in preparing the powder mixtures required for the fabrication of ZrB_2 + SiC UHTCs typically involves attrition or planetary milling in wet conditions of the ZrB_2 and SiC starting powders either together or separately (in the latter case, there is a later additional step of homogenization) for

* Corresponding author. Tel.: +34 924289600x86726; fax: +34 924289601.
E-mail addresses: alortiz@materiales.unex.es, alortiz@unex.es (A.L. Ortiz).

0955-2219/$ – see front matter © 2011 Elsevier Ltd. All rights reserved.
doi:10.1016/j.jeurceramsoc.2011.05.035

24 h or more to refine the particle sizes, followed by drying the slurries.[3–16] This approach results in sinterable, homogeneous mixtures of ZrB_2 plus SiC powders, but with sub-micrometre particle sizes (i.e., ~0.5 μm) because under these operating conditions attrition or planetary milling is a form of conventional milling. While the benefits of this processing strategy over the use of pure ZrB_2 are indisputable, the processing routine would be markedly simplified and the sinterability would be further improved if the ZrB_2 and SiC powders were refined together directly down to nanoscale. This cannot be achieved by conventional ball-milling, however, because the stresses generated are not high enough to fracture fine particles. Recently, it has been shown that high-energy ball-milling (HEBM) in dry conditions with shaker millers can produce ultrafine agglomerates (i.e., ~120 nm) of nano-particles (i.e., ~15 nm) from pure ZrB_2 powders in a few hours.[17] But the procedure is not directly extrapolatable to mixtures of ZrB_2 and SiC powders because it is unknown whether the addition of a second phase such as SiC affects the HEBM comminution mechanism of ZrB_2 or its kinetics. This therefore was the target of the present study which is aimed at comparing the HEBM behaviour of ZrB_2 without and with different additions (5, 17.5, and 30 vol.%) of SiC. We found that ZrB_2 is not immune to the presence of SiC, and discuss the implications that this has for the preparation of nano-powders of ZrB_2 plus SiC.

2. Experimental procedure

Commercially available powders of ZrB_2 and SiC (in both cases Grade B of H.C. Starck, Berlin, Goslar, Germany) were used as starting materials. The SiC is of type α, in particular, essentially the 6H polytype.[18] The two as-purchased powders have a >99.5% purity, and consist of single-crystal particles with an average size of ~2 μm in the case of ZrB_2 and ~0.55 μm in the case of SiC. Four powder compositions were prepared: pure ZrB_2, and ZrB_2 plus 5, 17.5, and 30 vol.% SiC (abbreviated henceforth as ZrB_2–x%SiC, where x refers to the vol.% SiC content). The HEBM of the pure ZrB_2 powders and of the three ZrB_2 + SiC powder mixtures was performed using a shaker mill (Spex D8000, Spex CertiPrep, Metuchen, NJ) equipped with cylindrical hardened-steel containers loaded with 5 WC/Co balls of 6.7 mm in diameter. The milling was carried out by shaking the containers at about 1060 back-and-forth cycles per minute in a complex three-dimensional trajectory, under the following conditions: ball-to-powder weight ratio of 4, and milling times in the range 1–180 min in air to impart different degrees of milling intensity.

The as-purchased and ball-milled powders were characterized using X-ray diffractometry (XRD), laser scattering (LS), and field-emission scanning electron microscopy (FE-SEM). The XRD was used to identify the phases present, to determine the phase composition in selected cases, and to evaluate the crystallite size of ZrB_2 as a function of the ball-milling condition. The phase identification was performed by indexing the XRD patterns with the aid of the PDF2 database. The phase composition was determined quantitatively by Rietveld analysis of the XRD patterns, using the commercial software package Topas (Topas 4.1, Bruker AXS, Karlsruhe, Germany).[19] The crystallite sizes of ZrB_2 were evaluated by applying the variance method[20] to its 1 0 1 peak. This peak was chosen because it is the most intense one of ZrB_2, and does not overlap with any SiC peak. The crystallite size of SiC in the ZrB_2 + 30%SiC mixture was evaluated from its 1 0 3 peak, which is intense, does not overlap with any ZrB_2 peak, and is located near the 1 0 1 peak of ZrB_2. The XRD data were collected in step-scanning mode with monochromatic Cu $K\alpha_1$ radiation (λ = 1.54183 Å), using a high-resolution laboratory diffractometer (D8 Advance, Bruker AXS, Karlsruhe, Germany) and the following three acquisition conditions: (1) scanning in the range 20–80° 2θ, step width 0.016° 2θ, and count time 3 s/step which was used to identify the phases present, (2) scanning in the range 39.5–44.5° 2θ, step width 0.016° 2θ, and count time 5 s/step which was used to evaluate the ZrB_2 crystal sizes, and (3) scanning in the range 36.5–39.5° 2θ, step width 0.016° 2θ, and count time 15 s/step which was used to evaluate the SiC crystal sizes. The LS was used to determine the particle sizes in the powders, with the analyzer employed being equipped with red and blue light sources (Mastersizer 2000, Malvern Instruments, Worcestershire, UK). These determinations were performed in quintuplicate. The FE-SEM was used to examine the particle morphology, and to validate the particle and crystallite sizes measured by LS and XRD, respectively. The observations were made without metal coating, at 10 kV with secondary electrons, using a field-emission microscope (S4800-II, Hitachi, Ibarakiken, Japan). The XRD, LS, and FE-SEM specimens were prepared using routine methods applicable to ceramic powders.

3. Results

Fig. 1 shows XRD patterns of the pure ZrB_2 powders and of the ZrB_2 + 30%SiC mixture before and after HEBM for selected times. Since the XRD patterns of the ZrB_2 + 5%SiC and ZrB_2 + 17.5%SiC mixtures showed the same trends as those that will now be discussed for the extreme cases of the pure ZrB_2 powder and the ZrB_2 + 30%SiC mixture, they will not be presented for the sake of brevity. It can be seen in Fig. 1 that the XRD peaks are increasingly broader and lower with increasing HEBM time. Because of the absence of severe plastic deformation in the brittle ZrB_2 and SiC,[17,21] the broadening and collapse of the peaks indicate that HEBM progressively refines the crystallite sizes. It can also be seen in Fig. 1 that the XRD peaks do not shift from their position in the un-milled condition, indicating that HEBM neither alters the crystal structures nor forms solid solutions between the ZrB_2 and SiC in the case of the ZrB_2 + SiC mixtures. Finally, in Fig. 2 one observes that the XRD patterns after 180 min of HEBM exhibit WC peaks, indicating contamination of the powders by the milling media at some time between 60 and 180 min of HEBM. The level of contamination is very low, however, with the Rietveld analysis of the XRD patterns (included in Fig. 2) showing that the WC content after 180 min of HEBM is less than 2.5 wt.%. This minute contamination by WC had been not observed in previous studies of HEBM on ZrB_2,[17,22] and was probably detected in the present

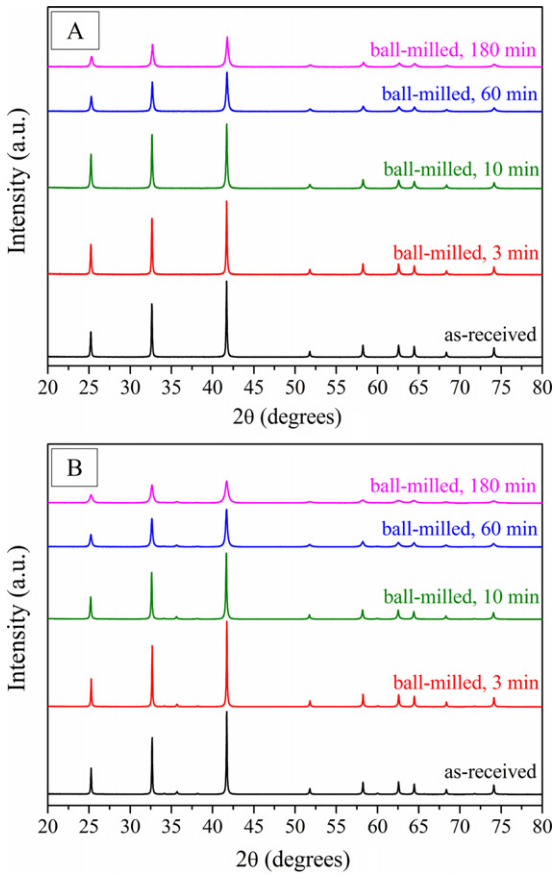

Fig. 1. XRD patterns of (A) the ZrB_2 powders and of (B) the ZrB_2 powders with 30 vol.% of SiC before and after HEBM for selected times.

study thanks to the use of a high-resolution diffractometer. The contamination by WC, however, should not be interpreted as a negative aspect because WC itself is a sintering additive of ZrB_2.[23]

Fig. 3 shows the average crystallite size of ZrB_2 as a function of the HEBM time in the powders milled in the pure state and co-milled with SiC (5, 17.5, or 30 vol.%). It can be seen that

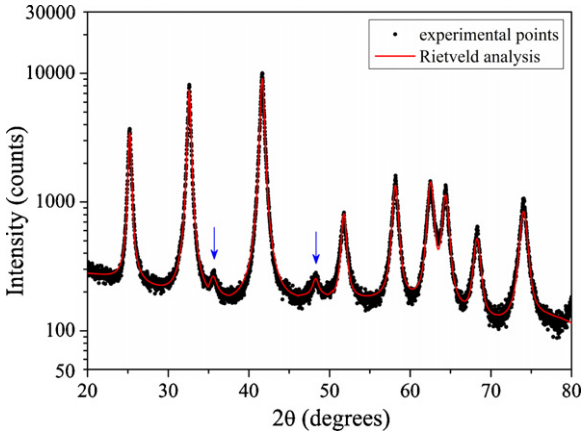

Fig. 2. XRD pattern of the ZrB_2 powder after 180 min of HEBM, together with the corresponding Rietveld analysis. The WC peaks free of overlap with ZrB_2 peaks are marked with arrows. The logarithmic scale is to facilitate the appreciation of the WC peaks.

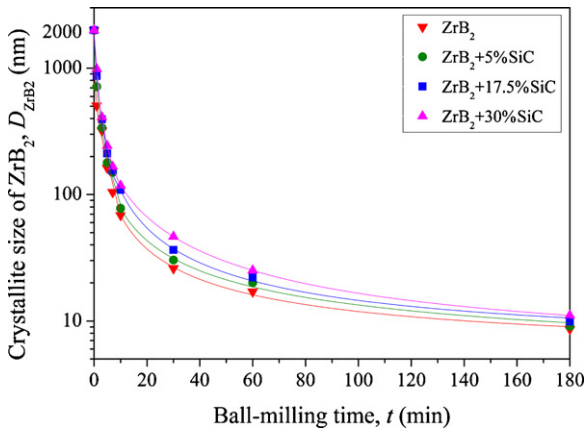

Fig. 3. Average crystallite size of ZrB_2 as a function of HEBM time for the ZrB_2 powders ball-milled without and with SiC (5, 17.5, and 30 vol.%). The solid lines are to guide the eye. The crystallite size in the as-purchased condition was taken to be the same as the particle size.

the evolution of the crystallite size with HEBM time is qualitatively similar in all cases, i.e., the crystallite size first decreases rapidly, then much more gradually, and finally tends asymptotically towards a certain limiting value. It is also very evident in Fig. 3, however, that ZrB_2 crystals are refined more slowly when they are co-milled with SiC, an effect that becomes more pronounced with increasing SiC load in the ZrB_2 + SiC mixture. Thus, for example, using the expression $D = Kt^{2/3}$ to model the dependence of crystallite size on the HEBM time,[24,25] the constant K is found to be 513 ± 30 nm min$^{2/3}$ for the ZrB_2 powder without SiC, and 672 ± 34, 807 ± 43, and 903 ± 51 nm min$^{2/3}$ for the powders with 5, 17.5 and 30 vol.% SiC, respectively. The addition of SiC, however, did not alter the limiting crystallite size because if the curves are extrapolated to longer HEBM time, they all appear to converge at ~5 h of ball-milling at a crystallite size of ~7–8 nm. Finally, the ZrB_2 crystallites are in all cases free of lattice microstrains and have the same lattice parameters as in the as-received condition because the XRD analysis revealed no signs of Gaussian peak broadening or peak shifting.

Fig. 4 compares FE-SEM images of the typical particles in the pure ZrB_2 powder milled for short and long times. One observes in Fig. 4A that the particle size of the starting powder (~2 μm) is rapidly reduced to the sub-micrometre scale in less than 1 min of HEBM, and that the powder particles have faceted surfaces. Furthermore, as in the case shown in this Fig. 4A, some of these particles contain cracks. After long-term HEBM (Fig. 4B), the morphology of the powder particles has evolved towards smooth-surfaced nano-particles (i.e., <20 nm) that form ultrafine (i.e., <200 nm in size) agglomerates. Furthermore, TEM observations performed by us in previous studies of HEBM on ZrB_2 (not repeated here) have shown that these agglomerates are indeed porous and that their primary nano-particles are crack-free.[17] Finally, the fact that these agglomerates are strong, because they have survived the ultrasonic bath, reveals the occurrence of cold-welding. Cold-welding during HEBM is a well-known phenomenon, and is typical but not exclusive of ductile compounds.[24,26] Indeed, despite the brittleness of ZrB_2, cold-welding occurs for long HEBM times because nano-

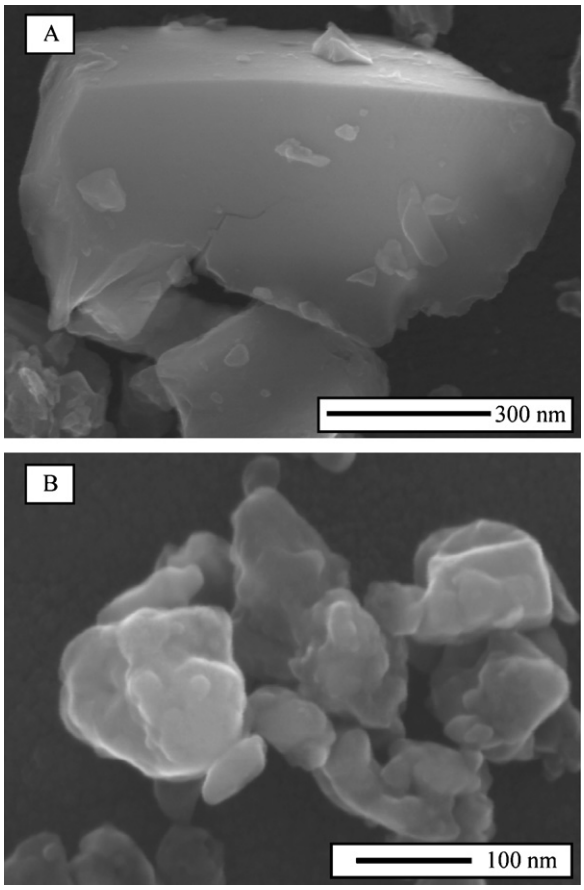

Fig. 4. FE-SEM images of the ZrB_2 powder particles after HEBM for (A) 1 min and (B) 180 min.

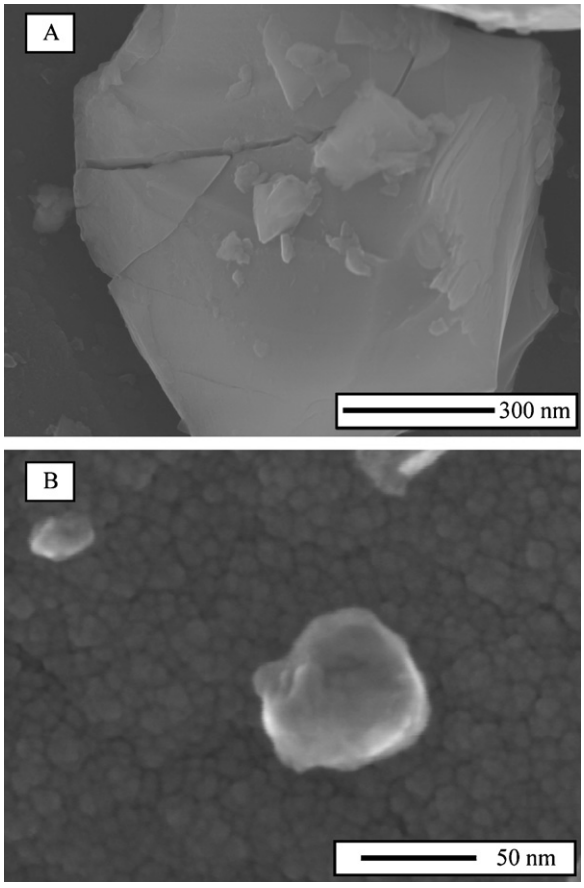

Fig. 5. FE-SEM images of the powder particles in the ZrB_2 powder with 30 vol.% of SiC after HEBM for 1 min showing the presence of (A) micrometre-sized particles (ZrB_2) and (B) nano-particles (SiC).

particles behave in a more ductile fashion, and there is a local temperature spike at the collision site (~300–500 °C) with the presence of high compressive stresses (~6 GPa) of very short duration (of the order of 10^{-6}–10^{-5} s).[26]

Fig. 5 shows FE-SEM images of the typical particles in the ZrB_2 + 30%SiC mixture milled for only 1 min. Unlike the pure ZrB_2 powder, the ZrB_2 + 30%SiC mixture consists of two distinct types of particle, one of sub-micrometre sizes (Fig. 5A) and the other of nanometre sizes (Fig. 5B). The extensive FE-SEM observations showed the sub-micrometre particles to be very abundant, to typically have sizes ranging from 1 to 0.3 μm, to have faceted surfaces, and (as in the case shown) to sometimes contain cracks. They also indicated that the less abundant nano-particles are smaller than 100 nm, have rounded surfaces, and are randomly distributed between the sub-micrometre particles. The EDS analysis performed during the FE-SEM examinations revealed that in general the sub-micrometre particles are ZrB_2 and the nano-particles are SiC. There are also some small ZrB_2 particles with angular shapes. These are fracture debris of the larger ZrB_2 particles. As in the case of the pure ZrB_2 powder, the FE-SEM image in Fig. 6 shows that long-term HEBM also changes the morphology of the particles in the ZrB_2 + 30%SiC mixture to strong agglomerates that have much finer, rounded particles which are cold-welded in their interior. When ZrB_2 is co-milled with SiC, these agglomerates are somewhat smaller, and their primary particles are somewhat larger. Thus, the addition of SiC slows down the kinetics of crystallite size refinement (see Fig. 3) and minimizes the cold-welding of the ZrB_2 particles during HEBM. Furthermore, the EDS analysis of the agglomerates in the ZrB_2 + 30%SiC powder mixture showed the predominance of Zr accompanied by smaller amounts of Si. This chemical analysis result was found to be quite reproducible from

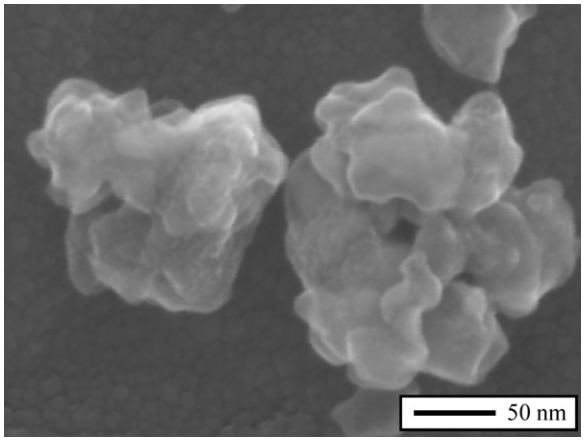

Fig. 6. FE-SEM images of the powder particles in the ZrB_2 powder with 30 vol.% of SiC after HEBM for 180 min.

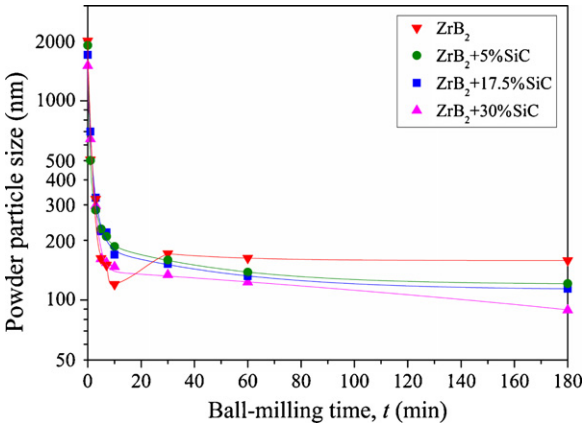

Fig. 7. Average powder particle size as a function of HEBM time for the ZrB_2 powders ball-milled without and with SiC (5, 17.5, and 30 vol.%). The solid lines are to guide the eye.

one agglomerate to other. These observations, together with the previous XRD analysis that ruled out the formation of solid solutions, indicate that these agglomerates are composed of individual nano-particles of ZrB_2 and SiC homogeneously mixed at a nanometre scale.

Fig. 7 shows the average size of the particles as a function of the HEBM time in the powders milled in the pure state and co-milled with SiC (5, 17.5. or 30 vol.%). There are various interesting features in this figure. Firstly, the evolution of the particle size is substantially different in the powders milled with and without SiC. In the case of the pure ZrB_2 the particle size first decreases, then increases, and finally stabilizes, whereas in the ZrB_2 + SiC mixtures the particle size decreases continuously. Secondly, the particle sizes determined by LS in the ZrB_2 + SiC mixtures at the early stages of HEBM are smaller than the crystallite sizes of ZrB_2 measured by XRD, unlike the case of the pure ZrB_2 powder. Furthermore, the particle sizes in the ZrB_2 + SiC mixtures do not follow the increasing trend of the crystallite sizes with increasing the SiC loading shown in Fig. 3. The clear explanation of these two observations is that at short HEBM times the SiC particles are much smaller than the ZrB_2 particles (i.e., nanometre *vs* sub-micrometre sizes; Fig. 5A and B), and that LS measures the contributions from both ZrB_2 and SiC whereas XRD distinguishes them. Thirdly, LS always yields far larger sizes than XRD in the late stages of HEBM. This is simply due to the formation of hard agglomerates, as was observed by FE-SEM (Figs. 4B and 6). The LS data thus confirm the occurrence of cold-welding during HEBM in all cases, and also show it to be much less severe with increasing SiC content (ultimate agglomerate sizes of 160, 120, 115, and 90 nm for SiC loads of 0, 5, 17.5, and 30 vol. %, respectively).

4. Discussion

The XRD, FE-SEM, and LS results presented above demonstrate that the behaviour of the crystallite size refinement of ZrB_2 has been altered by the presence of SiC. Specifically, high-energy co-ball-milling of ZrB_2 with SiC does not change the mechanism of crystallite size refinement, but slows down its kinetics. This conclusion is inferred from the fact that the crystallite size curves of ZrB_2 in Fig. 3 all obey the same functional dependence on HEBM time (i.e., $D = Kt^{2/3}$), but with the constant K increasing with the SiC content. The mechanism is repeated brittle fracture followed by cold-welding, as revealed by the following experimental observations: (i) the rapid refinement in the early stages of HEBM and the existence of a limiting crystallite size, (ii) the faceted shape and the cracks in the powder particles at short HEBM times, (iii) the absence of lattice microstrains in the interior of the crystals throughout the HEBM that rules out severe plastic deformation, and (iv) the formation of strong agglomerates containing primary nano-particles in the late stages of HEBM. Although SiC does not change the mechanism of crystallite size refinement, it does have two distinct effects: (i) reducing the rate of crystallite size refinement, and (ii) promoting the formation of finer agglomerates. The former phenomenon is a surprise to us because it is not what we would have expected. Previous studies[22,27] have revealed that adding a softer material during ball-milling slows down the crystallite size refinement of the harder material because the softer material can act as a lubricant. When a harder material is added, such as adding SiC to Al, the crystallite size refinement of the softer material accelerates substantially due to the increased severe plastic deformation of the softer material induced by the presence of many harder material particles.[28,29] SiC is harder than ZrB_2; however, as shown in this study, it does not accelerate the crystallite size refinement of ZrB_2, indicating that a new mechanism is present for the ZrB_2 + SiC mixture. This new mechanism is discussed below.

One of the possible mechanisms for the unexpected effect of SiC discussed above is the reduced ball-to-powder volume ratio with the addition of SiC to ZrB_2. We have shown in an earlier study[17] that the crystallite size refinement of pure ZrB_2 is slower when the ball-to-powder weight ratio is reduced from 4 to 2, equivalent to ball-to-powder volume ratios of 1.6 and 0.8, respectively. Using the ball-to-powder weight ratio of 4, the total volume of the WC balls, and the density values of ZrB_2 (6.1 g cm^{-3}) and SiC (3.21 g cm^{-3}) together with their concentrations, one calculates the ball-to-powder volume ratio to be 1.6, 1.56, 1.35, and 1.33 for the pure ZrB_2 powder and the ZrB_2 + 5%SiC, ZrB_2 + 17.5%SiC, and ZrB_2 + 30%SiC mixtures, respectively. This straightforward calculation shows that the ball-to-powder volume ratio decreased with increasing SiC concentration in the ZrB_2 + SiC mixture simply because we maintained the ball-to-powder weight ratio fixed at 4 and ZrB_2 is denser than SiC. It might then be argued that the slower crystallite size refinement of ZrB_2 with increasing SiC concentration in the ZrB_2 + SiC mixtures is due simply to this decrease in the ball-to-powder volume ratio, thereby reducing the effective compressive stresses applied to the individual particles during HEBM. However, as shown in Fig. 8, when one compares the data of crystallite size as a function of HEBM time for the pure ZrB_2 ball milled with a ball-to-powder volume ratio of 0.8[17] and the ZrB_2 + 30%SiC ball-milled with a ball-to-powder volume ratio of 1.33, one finds that the kinetics of crystallite size refinement is slightly slower for the latter despite the fact that the ball-to-powder volume ratio is much higher (i.e., 67%

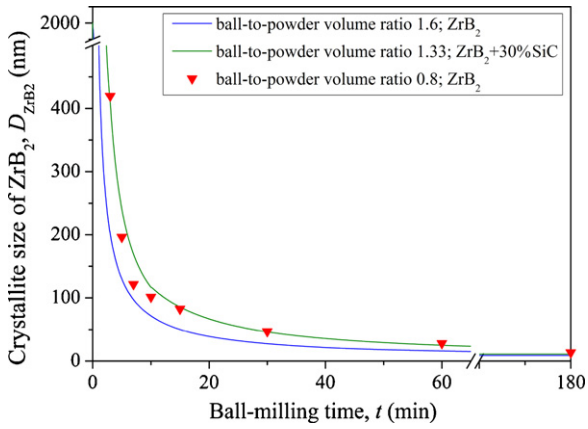

Fig. 8. Average crystallite size of ZrB_2 as a function of HEBM time for the ZrB_2 powders ball-milled without SiC using ball-to-powder volume ratios of 1.6 and 0.8, and with 30 vol.% of SiC using a ball-to-powder volume ratio of 1.33.

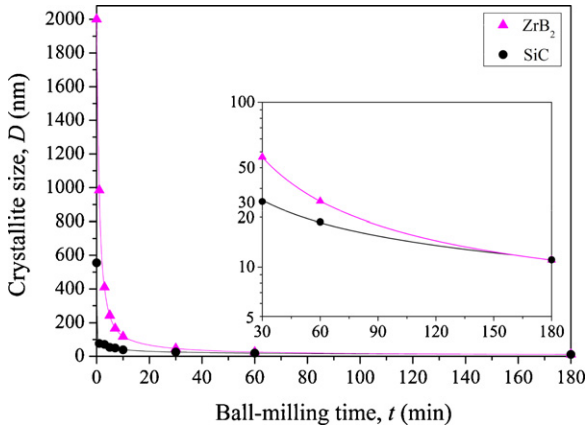

Fig. 9. Average crystallite size of ZrB_2 and SiC as a function of HEBM time for the ZrB_2 powders ball-milled with 30 vol.% of SiC. The solid lines are to guide the eye. The inset is a detail of the region of long-duration HEBM.

higher). Thus, this comparison clearly rules out the mechanism of reducing the ball-to-powder volume ratio played by SiC.

Another possible mechanism for the unexpected effect of SiC is the reduction of the crystallite size refinement rate through the direct role played by SiC. A previous study[22] has shown that the slower kinetics of crystallite size refinement during the HEBM of ZrB_2 can be achieved in the presence of 2 wt% graphite. This phenomenon has been attributed to the lubricating effect of the graphite on the contacts between the ZrB_2 particles themselves as well as between the particles and the colliding balls. Thus, SiC may, like graphite, also "lubricate" the contacts during the HEBM of ZrB_2. However, unlike graphite, SiC has no lubricating properties by itself, and the coefficients of friction of SiC and ZrB_2 in dry air are very similar (~0.8).[30,31] Therefore, the "lubrication" mechanism has necessarily to be different. The evidence obtained by FE-SEM (Fig. 5B) suggested that this mechanism may well be closely related to the nanoscale size of SiC. We therefore monitored by XRD the evolution of the SiC crystals in the $ZrB_2 + 30\%$SiC mixture throughout the HEBM, and compared it with that of the ZrB_2 crystals in the same mixture (Fig. 9).[a] It can be seen that the general trend is qualitatively similar, and can also be described by the expression $D = Kt^{2/3}$ because the mechanism of crystal size refinement is the same in SiC as in ZrB_2. However, the crystallite size refinement of SiC is much faster than that of ZrB_2, with the constant K being $103 \pm 8\,\text{nm}\,\text{min}^{2/3}$ for SiC *vs* the $903 \pm 51\,\text{nm}\,\text{min}^{2/3}$ for ZrB_2. Thus, despite its smaller particle size in the as-purchased condition which would make fracture more difficult, SiC is refined faster than ZrB_2 due to its greater brittleness (K_{IC} of 3 *vs* 5 $\text{MPa}\,\text{m}^{1/2}$). The important feature to note in Fig. 9 is that the particle size of the SiC starting powder (0.55 μm) is reduced rapidly to below 100 nm in less than 1 min of HEBM, after which the further reduction in crystallite size is very slight. We believe that this early nano-crystallization of SiC is the key to the unexpected effect of SiC. Crystallite size refinement in brittle materials occurs by brittle fracture, and fracture strength scales inversely with the square root of the crystal sizes.[32] This accounts for the $t^{-2/3}$ dependence of the crystal size on the HEBM time. At a certain critical HEBM time, the crystals have became small enough, i.e., nanoscale, for the compressive stress imparted during the collisions to fall below the crystals' fracture strength. These nano-crystals, once formed, can no longer be fractured during HEBM, and consequently simply slide past each other because the collisions during the HEBM occur without lateral constraints. In this scenario, the SiC nano-crystals consume collision energy and reduce the compressive stress on ZrB_2 particles. As a result, crystallite size refinement of ZrB_2 slows down and harder SiC appears to have the "lubricating" effect. This energy consumption mechanism is also consistent with the phenomenon of increasing SiC load leading to slower refinement kinetics (Fig. 3). The fact that the presence of SiC does not affect the ultimate size of the ZrB_2 crystallites (Fig. 3) is also in good agreement with this mechanism because the ultimate size is mainly determined by the fracture strength of the crystallites and the compressive stress at the collision site.

It is interesting to note that the generation of many SiC nanoparticles at the early stage of HEBM is in good accordance with the observation that the more SiC, the finer agglomerates (Fig. 7). It is well known that the size of agglomerates is determined by the combined effect of the fracture rate and the cold-welding rate.[24] For pure ZrB_2 the fracture rate is high at the early stage of HEBM, leading to the formation of the smallest agglomerates at about 10-min of HEBM (Fig. 7). However, as the HEBM time increases, the fracture rate decreases because smaller particle sizes are more resistant to fracture[32] and the cold-welding rate increases due to the increased number of particles. As a result, the size of agglomerates increases and finally stabilizes as the HEBM time increases beyond 10 min (Fig. 7).

For the $ZrB_2 + SiC$ mixtures both the fracture rate and the cold-welding rate are altered by SiC. Fundamentally, the extent of cold-welding and its rate during HEBM of multiple brittle materials are affected by the chemical affinity between different

[a] The choice of the $ZrB_2 + 30\%$SiC mixture powder for this purpose was simply because the greater SiC content facilitates the precise modeling of the SiC XRD peaks required to accurately calculate its crystallite size.

materials. As evidenced by the smaller agglomerate sizes for all of the ZrB_2 + SiC mixtures in comparison with the pure ZrB_2 powder, the present study has revealed that the chemical affinity between SiC and ZrB_2 is lower than that between ZrB_2 themselves at the HEBM temperature. Based on this reasoning, the observed alternation in the agglomerate size as a function of the HEBM time for the ZrB_2 + SiC mixtures can be explained as follows. At the early stage of HEBM, the fracture rate of ZrB_2 has been reduced because of the collision energy consumption by frictional sliding of many SiC nano-particles and thus the reduced compressive stress on ZrB_2 particles. The reduced fracture rate results in larger agglomerate sizes than those observed for the pure ZrB_2 powder at the early stage of HEBM (Fig. 7). However, as the HEBM time increases and most of the ZrB_2 particles become very small, the major role of SiC nano-particles changes to minimize cold-welding events because of the lower chemical affinity between SiC and ZrB_2 than that between ZrB_2 themselves at the HEBM temperature. As a result, when more SiC is added and thus more SiC nano-particles are trapped at the collision site, fewer ZrB_2 can be cold-welded, leading to the phenomenon that the more SiC, the finer agglomerates at the long HEBM time (Fig. 7).

Finally, the present study has interesting implications concerning the processing of ZrB_2 + SiC UHTCs. Firstly, relative to the conventional attrition milling of ZrB_2 + SiC mixtures, the refinement of the primary particle sizes to the nanoscale achieved by HEBM is expected to enhance the subsequent sintering kinetics if powder pressing is conducted properly. Such expected enhancement is due to the reduced diffusion distance and increased interparticle interfaces resulting from the formation of ultrafine agglomerates composed of primary nano-particles. Secondly, the processing routine is simplified notably both by the elimination of steps during the powder batch preparation, and by the time-saving in other steps due to the high-energy co-ball-milling in dry conditions dealing simultaneously with the ZrB_2 refinement and the homogeneous dispersion of the SiC additive at nanometre scale in a few hours. Indeed, these are objectives which have been extensively pursued by the UHTC community.

5. Conclusions

The effect has been investigated of SiC addition on the HEBM behaviour of the ZrB_2 powders used to process UHTCs. The results allow the following conclusions to be drawn:

1. The presence of SiC during HEBM does not change the comminution mechanism of ZrB_2, i.e., repeated brittle fracture followed by cold-welding. With this mechanism, the powder particles formed during HEBM are first sub-micrometre single-crystals, and then become ultrafine agglomerates consisting of single-crystal nano-particles.
2. The SiC addition, however, does slow down the refinement kinetics of the ZrB_2 crystals and decreases cold-welding, promoting the formation of finer agglomerates. The former is attributed to the early nano-crystallization of SiC during HEBM and the collision energy consumption by frictional sliding of SiC nano-particles, leading to lower compressive stresses on ZrB_2 particles. The latter is due to the lower chemical affinity between SiC and ZrB_2 than ZrB_2 themselves and the generation of many SiC nano-particles at the early stage of HEBM.
3. The SiC addition does not affect the ultimate crystal size of ZrB_2 because this is mainly dictated by the fracture strength and by the compressive stress at the collision site.
4. The addition of a harder material with a lower fracture toughness (e.g., SiC) than the softer material (e.g., ZrB_2) can slow down the refinement of crystallite sizes. This discovery offers a new mechanism to control the crystallite size during HEBM in the future.
5. High-energy co-ball-milling offers an exciting opportunity to attain ultrafine nano-agglomerates consisting of ZrB_2 and SiC nano-particles intimately dispersed at a nanoscale, factors which would be expected to facilitate the sintering of the ZrB_2–SiC composites. This, together with the simplification of the powder preparation routine, suggests that high-energy co-ball-milling may have an important role to play in the processing of ZrB_2–SiC UHTCs.

Acknowledgement

This work was supported by the Ministerio de Ciencia y Tecnología (Government of Spain) under Grant N° MAT 2007-61609.

References

1. Fahrenholtz WG, Hilmas GE, Talmy IG, Zaykoski JA. Refractory diborides of zirconium and hafnium. *J Am Ceram Soc* 2007;**90**(5):1347–64. See also references therein.
2. Guo S-Q. Densification of ZrB_2-based composites and their mechanical and physical properties: a review. *J Eur Ceram Soc* 2009;**29**(6):995–1011. See also references therein.
3. Hwang SS, Vasiliev AL, Padture NP. Improved processing and oxidation resistance of ZrB_2 ultra-high temperature ceramics containing SiC nanodispersoids. *Mater Sci Eng A* 2007;**464**(1–2):216–24.
4. Chamberlain AL, Fahrenholtz WG, Hilmas GE, Ellerby DT. High-strength zirconium diboride-based ceramics. *J Am Ceram Soc* 2004;**87**(6):1170–2.
5. Yan Y, Huang Z, Dong S, Jiang D. Pressureless sintering of high-density ZrB_2–SiC ceramic composites. *J Am Ceram Soc* 2006;**89**(11):3589–92.
6. Zhu S, Fahrenholtz WG, Hilmas GE. Influence of silicon carbide particle size on the microstructure and mechanical properties of zirconium diboride-silicon carbide ceramics. *J Eur Ceram Soc* 2007;**27**(4):2077–83.
7. Zhang SC, Hilmas GE, Fahrenholtz WG. Pressureless sintering of ZrB_2–SiC ceramics. *J Am Ceram Soc* 2008;**91**(1):26–32.
8. Monteverde F, Bellosi A, Scatteia L. Processing and properties of ultra-high temperature ceramics for space applications. *Mater Sci Eng A* 2008;**485**(1–2):415–21.
9. Zou J, Zhang G-J, Kan Y-M, Wang P-L. Pressureless densification of ZrB_2–SiC composites with vanadium carbide. *Scripta Mater* 2008;**59**(3):309–12.
10. Zhang SC, Hilmas GE, Fahrenholtz WG. Mechanical properties of sintered ZrB_2–SiC ceramics. *J Eur Ceram Soc* 2009;**31**(5):893–901.
11. Watts J, Hilmas G, Fahrenholtz WG, Brown D, Clausen B. Stress measurements in ZrB_2–SiC composites using raman spectroscopy and neutron diffraction. *J Eur Ceram Soc* 2009;**30**(11):2165–71.
12. Zhang H, Yan Y, Huang Z, Liu X, Jiang D. Properties of ZrB_2–SiC ceramics by pressureless sintering. *J Am Ceram Soc* 2009;**92**(7):1599–602.

13. Guo W-M, Zhang G-J, Wang P-L. Microstructural evolution and grain growth kinetics in ZrB_2–SiC composites during heat treatment. *J Am Ceram Soc* 2009;**92**(11):2780–3.
14. Wang X-G, Guo W-M, Zhang G-J. Pressureless sintering mechanism and microstructure of ZrB_2–SiC ceramics doped with boron. *Scripta Mater* 2009;**61**(2):177–80.
15. Zhang H, Yan Y, Huang Z, Liu X, Jiang D. Pressureless sintering of ZrB_2–SiC ceramics: the effect of B_4C content. *Scripta Mater* 2009;**60**(7):599–662.
16. Zamora V, Sánchez-González E, Ortiz AL, Miranda P, Guiberteau F. Hertzian indentation of a ZrB_2–30%SiC ultra-high-temperature ceramic up to 800 °C in air. *J Am Ceram Soc* 2010;**93**(7):1848–51.
17. Galán CA, Ortiz AL, Guiberteau F, Shaw LL. Crystallite size refinement of ZrB_2 by high-energy ball milling. *J Am Ceram Soc* 2009;**92**(12):3114–7.
18. Xu H, Bhatia T, Deshpande SA, Padture NP, Ortiz AL, Cumbrera FL. Microstructural evolution in liquid-phase-sintered SiC. Part I. Effect of starting powder. *J Am Ceram Soc* 2001;**84**(7):1578–84.
19. Coelho A. TOPAS Academic, Version 4. Bruker AXS; 2000.
20. Sánchez-Bajo F, Ortiz AL, Cumbrera FL. Analytical formulation of the variance method of line-broadening analysis for voigtian X-ray diffraction peaks. *J Appl Crystallogr* 2006;**39**(4):598–600.
21. Pan YB, Huang ZR, Jiang DL, Mazerolles L, Michel D, Pastol J-L, et al. High energy planetary ball milling of SiC powders. *Key Eng Mater* 2007;**351**:7–17.
22. Galán CA, Ortiz AL, Guiberteau F, Shaw LL. High-energy ball milling of ZrB_2 in the presence of graphite. *J Am Ceram Soc* 2010;**93**(10):3072–5.
23. Chamberlain AL, Fahrenholtz WG, Hilmas GE. Pressureless sintering of zirconium diboride. *J Am Ceram Soc* 2006;**89**(2):450–6.
24. Suryanarayana C. Mechanical alloying milling. *Prog Mater Sci* 2001;**46**(1–2):1–184.
25. Li S, Wang K, Sun L, Wang Z. A simple model for the refinement of nanocrystalline grain size during ball milling. *Scripta Metall Mater* 1992;**27**(4):437–42.
26. Soni PR. *Mechanical alloying, fundamental and applications*. Cambridge, UK: Cambridge International Science Publishing; 2001.
27. Shaw L, Yang Z-G, Ren R-M. Synthesis of nanostructured Si_3N_4/SiC composite powders through high energy reaction milling. *Mater Sci Eng A* 1998;**244**(1):113–26.
28. Saberi Y, Zebarjad SM, Akba GH. On the role of nano-size SiC on lattice strain and grain size of Al/SiC nanocomposite. *J Alloys Compd* 2009;**484**(1–2):637–40.
29. Kamrani S, Simchi A, Riedel R, Seyed-Reihani SM. Effect of reinforcement volume fraction on mechanical alloying of Al–SiC nanocomposite powders. *Powder Metall* 2007;**50**(3):276–82.
30. Lu Z, Zhou Y, Zhang M, Huang Q. Dry friction behaviour of reaction-bonded silicon carbide at high temperature. *Key Eng Mater* 1993;**336–338**:2472–4.
31. Umeda K, Enomoto Y, Mitsui A, Mannami K. Friction and wear of boride ceramics in air and water. *Wear* 1993;**169**(1):63–8.
32. Lawn BR. *Fracture of brittle solids*. Cambridge, UK: Cambridge University Press; 1993.